


# Preparation of Antimicrobial Iron Oxide Nanostructures from Galvanizing Effluent

Rajapakse Babilage Sanjitha Dilan Rajapakshe<sup>1,2\*</sup> ,  
Gonapaladeniya Madhusa Chathurangi Gonapaladeniya<sup>1,2</sup>,  
Charith Anuruddha Thennakoon<sup>1,2</sup>, Prabath Nilan Gunasekara<sup>3</sup>,  
Nirosh Siriwardene<sup>3</sup>, Sudath Annasiwatte<sup>3</sup>, Sayuri Sammanani Niyangoda<sup>1</sup>,  
Rajapakse Mudiyansele Gani Rajapakse<sup>1,2</sup>

<sup>1</sup>Department of Chemistry, Faculty of Science, University of Peradeniya, Peradeniya, Sri Lanka

<sup>2</sup>Post Graduate Institute of Science, University of Peradeniya, Peradeniya, Sri Lanka

<sup>3</sup>LTL Galvanizers Pvt. Ltd. Makola, Sri Lanka

Email: \*sandil.89@ku.edu

**How to cite this paper:** Rajapakse, R.B.S.D., Gonapaladeniya, G.D.M.C., Thennakoon, C.A., Gunasekara, P.N., Siriwardene, N., Annasiwatte, S., Niyangoda, S.S. and Rajapakse, R.M.G. (2022) Preparation of Antimicrobial Iron Oxide Nanostructures from Galvanizing Effluent. *World Journal of Nano Science and Engineering*, 12, 1-11.

<https://doi.org/10.4236/wjnse.2022.121001>

**Received:** February 27, 2022

**Accepted:** March 28, 2022

**Published:** March 31, 2022

Copyright © 2022 by author(s) and Scientific Research Publishing Inc. This work is licensed under the Creative Commons Attribution International License (CC BY 4.0).

<http://creativecommons.org/licenses/by/4.0/>



Open Access

## Abstract

Galvanization is the process of applying a protective zinc coating to iron or steel to prevent rusting. In the batch hot-dip galvanizing process, large amounts of wastes originate in liquid, solid and gaseous forms. Acidic waste containing iron and zinc ions is produced due to the cleaning of steel prior to zinc coating, which is considered the galvanizing acid waste. The galvanizing effluent used was collected from LTL Galvanizers Pvt. Ltd., Sapugaskanda, Sri Lanka, and converted into antimicrobial hematite ( $\alpha\text{-Fe}_2\text{O}_3$ ) nanoparticles. These nanoparticles were synthesized using a chemical precipitation method. X-Ray Diffraction (XRD) and Scanning Electron Microscopy (SEM) were used to characterize the nanomaterials produced. Two pathogenic bacteria and one pathogenic fungus were used to analyze the antimicrobial activity of the nanomaterials. All the samples showed excellent antibacterial and antifungal properties. And the material can inhibit the growth of both Gram-positive and Gram-negative bacteria. According to the SEM images, some of the hematite particles were around 100 nm in size or less, which confirms that the describing method is viable in synthesizing hematite nanostructures. As shown in the XRD, the major diffraction peak, located at  $2\theta$  of  $35.617^\circ$  (110) in addition to minor peaks at  $24.87^\circ$  (012),  $33.07^\circ$  (104),  $42.08^\circ$  (113),  $51.18^\circ$  (024),  $53.52^\circ$  (116) and  $57.46^\circ$  (018) confirm the spinel structure of iron oxide ( $\alpha\text{-Fe}_2\text{O}_3$ ). The estimated average crystallite size of the nanomaterial is calculated to be 36.74 nm. The durability of the manufactured nanomaterial is excellent. This method is a time-efficient, environmentally friendly, cost-effective and industrially viable way to manufacture antimicrobial hematite ( $\alpha\text{-Fe}_2\text{O}_3$ ) nanomaterials

from a galvanizing effluent.

## Keywords

Wastewater Treatment, Galvanizing Effluent, Antimicrobial Hematite Nanomaterials, Iron Oxide Nanostructures, Coprecipitation

---

## 1. Introduction

High strength and durability are two important characteristics of steel that enable its usage as an integral part of the building and construction industry [1] [2]. However, there is a major disadvantage of steel which is its corrosion when exposed to different external conditions. There are different methods to prevent corrosion of steel such as cathodic protection, anodic protection, the addition of inhibitors, protective coatings, and metallic coatings. Zinc coatings are extensively used for the protection of steel. In such cases, the more active zinc metal corrodes preferentially than the steel substrate by a cathodic reaction thereby preventing the steel from undergoing an anodic corrosion reaction [3] [4].

Different types of zinc coatings include hot dip galvanizing (batch or continuous), electroplating, metalizing (zinc spraying), mechanical plating, and zinc rich paint. Among them, the hot dip galvanization process offers a unique combination of superior properties such as high strength, formability, light weight, corrosion resistance, low cost, and recyclability [5]. Hot dip galvanizing is the process of coating iron or steel with a layer of zinc by immersing the metal in a bath of molten zinc at a temperature of around 450°C (842°F). During the process, a metallurgically bonded coating is formed which protects the steel from harsh environments, whether they be external or internal. [5] [6].

In the batch hot-dip galvanizing process a very acidic waste, containing iron and zinc is produced due to the cleaning of steel prior to zinc coating; this is considered the galvanizing acid waste. Presently the galvanizing process consists of neutralizing the acid with carbonates (limestone) or alkaline chemicals before being shipped off to a landfill as sludge [7] [8].

In this paper, we are discussing the process of how we used an industrial waste/effluent taken from LTL galvanizers, which pioneered the hot dip galvanizing method in Sri Lanka, to convert it into an antimicrobial nanomaterial using a simple chemical precipitation method. Waste generation is characteristic of any industrial process, and it requires treatment and/or appropriate disposal in compliance with environmental laws, giving priority to reuse rather than final disposal in landfills [9] [10]. Waste generated per month during the galvanizing process is huge. The acid waste is converted to a solid by adding limestone and then disposed of, which is an extra cost to the company, whereas piling up waste is an environmental threat. Therefore, converting the galvanizing effluent to a value-added product is beneficial and we decided to direct our attention toward iron oxide nanoparticle synthesis which then can be used for numerous other

applications.

Transition metals are considered the top candidates for the synthesis of metal-based nanoparticles since these have partially filled d-orbitals which make them more redox-active. This feature facilitates their nanoparticle aggregation [11]. There are several methods used to synthesize nanoparticles namely physical methods, chemical methods, and biological methods.

Advancement in modern medicines results in an increase in the utilization of metallic NPs for medical purposes due to their antibacterial, antiviral, antifungal, anti-inflammatory, and antiangiogenic properties [12]. Although the toxic antibacterial mechanism of metallic NPs is still under debate, three main mechanisms are proposed, which include, firstly, the formation of reactive oxidative species (ROS); secondly, releasing process of ions; and, finally, the interaction of NPs with the cell membrane [13]. The small-sized metallic NPs with larger surface areas exhibit some electronic effects which were beneficial to improving the surface attraction of NPs. In addition, the percentage of enhanced surface area straightly interacts with the membrane of microorganisms to a vast extent and hence bridged an improved relationship with bacteria. These two vital factors powerfully enhance the antimicrobial action of the NPs [14]. These NPs basically interact with soft bases, having sulfur or phosphorus components. So, the sulfur of proteins and phosphorus belonging to DNA molecules are favorite attacking sites of NPs. Then, these NPs attach themselves to enzymes (thiol groups), *i.e.*, nicotinamide adenine dinucleotide dehydrogenases (NADH) and destruct its respiratory chain by releasing reactive oxygen species, thus creating oxidative stress. Consequently, major damage is occurred to the cell structures and lastly leads to cell loss [15] [16].

In this paper we discuss a simple, cost effective and industrially viable method to synthesis anti-microbial iron oxide nanoparticles using a galvanizing effluent. The crystallographic structure of prepared nanostructures was analyzed using X-Ray Diffraction (XRD) and SEM images were used to determine the morphology of the material. Using two pathogenic bacteria Gram positive-*Staphylococcus aureus* (ATCC 25923), Gram negative *Escherichia coli* (ATCC 25922) and one pathogenic fungus *Candida albicans*, the antimicrobial activity of iron oxide nanoparticles was assessed by agar disc diffusion method.

## 2. Materials and Methods

### 2.1. Materials

The galvanizing effluent was collected from LTL Galvanizers, Sapugaskanda, Sri Lanka. All the other chemicals were purchased from Sigma Aldrich in analytical grade. Gram-positive, Gram-negative bacteria and fungi were obtained from the department of Microbiology, faculty of Medical Sciences, University of Sri Jayawardanapura, Colombo, Sri Lanka.

### 2.2. Preparation of Iron Oxide Nanoparticles

A series of samples were prepared with descending concentrations of effluent

precursor, as C1, C2, C3, C4 and C5 as shown below,

Sample No1 (C1)  $\rightarrow$  Fe<sup>3+</sup> in highest concentration/0.05 M;

Sample No2 (C2)  $\rightarrow$  C1/2;

Sample No2 (C3)  $\rightarrow$  C2/2;

Sample No2 (C4)  $\rightarrow$  C3/2;

Sample No2 (C5)  $\rightarrow$  C4/2.

Then the nanoparticles were synthesized by a chemical precipitation method, adding 1 M NaOH to a mixture of 0.01 M H<sub>2</sub>O<sub>2</sub> in a FeCl<sub>3</sub> solution (prepared using above mentioned effluent with different concentrations), while stirring vigorously using a magnetic stirrer till pH 9 (The ratio of ferrous (Fe<sup>2+</sup>), and ferric (Fe<sup>3+</sup>) present in the liquid effluent has been determined separately using a titration method to decide the amount of H<sub>2</sub>O<sub>2</sub> needed to be added in excess).

Then it was centrifuged at 4000 rpm for 10 minutes. After centrifugation, the supernatant was discarded, and the deposit was dissolved in fresh de-ionized water. This process was repeated until the supernatant became neutral in pH and the final deposit was collected into a clean watch glass. All the samples prepared with different precursor concentrations were cured separately at different temperatures, (100°C, 120°C and 140°C) for 20 minutes in a hot air oven and Iron Oxide (Fe<sub>2</sub>O<sub>3</sub>) nanoparticles were finally collected as power.

## 2.3. Characterization Techniques

### 2.3.1. X-Ray Diffraction (XRD)

To obtain the crystallographic structural information of the product, XRD pattern of finely ground NPs was observed under a wide range of Bragg's angles ( $\theta$ ) using a Siemens D5000 X-ray powder diffractometer operated at 40 kV and 30 mA current with Cu K $\alpha$  radiation ( $\lambda = 0.15419$  nm). Data were collected with a counting rate of 1°/min. The K $\alpha$  doublets were well resolved. The average crystallite size was calculated by Debye Scherrer formula.

### 2.3.2. Scanning Electron Microscope (SEM)

To characterize the mean particle size and morphology of Iron oxide nanoparticles, SEM was performed using a ZEISS EVO SEM machine of 20 KV of accelerating voltage.

### 2.3.3. Screening of Antimicrobial Activity

The antimicrobial activities of prepared nano materials were tested by the agar disc diffusion method. Two pathogenic bacteria, Gram positive-*Staphylococcus aureus* (ATCC 25923), Gram negative *Escherichia coli* (ATCC 25922) and one pathogenic fungus, *Candida albicans* were used in the process.

Mueller Hinton (MH) agar medium was used to cultivate bacteria. Fresh overnight cultures were taken and 100  $\mu$ L inoculum was spread uniformly over the agar medium using a sterile glass rod to get a consistent distribution of bacteria. These plates were labeled and a 25 mg patch of each nanoparticle materials (prepared with different precursor conditions) with a median diameter of 9 mm has added aseptically onto an agar plate. Then the plates were incubated for 24 h

at 37°C during which the activity was evidenced by the presence of an inhibition zone surrounding the patch. Antimicrobial activity was expressed as the size of the diameter of the inhibition zones (mm) produced by the nanoparticle around their vicinity.

### 3. Results and Discussion

1) Antibacterial activity results were obtained for the nanoparticles prepared with different concentrations at different temperatures

According to each of the above figures in **Figure 1** and **Table 1**, it can be identified that all the developed hematite samples have the anti-bacterial property to some extent around their vicinity. Having a very low anti-bacterial activity might be due to the availability of a low concentration of free radicals for the degradation of microbial cells. Still, the activity has increased to a greater extent in the samples developed with C4 precursor concentration than that of the results obtained with the samples from other precursor concentrations. This may be due to having smaller nanostructures with that specific precursor concentration at a higher availability. According to the “Blue-Shift” of the nanostructures, the band gap of the semiconductors increases with the decrease in particle size. Here as well, when the precursor concentration decreases the particle size of hematite nanostructures also decreases and their energy gap increases. With that, the energy of the excited electrons goes to higher values. Those electrons can easily convert the atmospheric oxygen to their respective “Reactive Oxygen

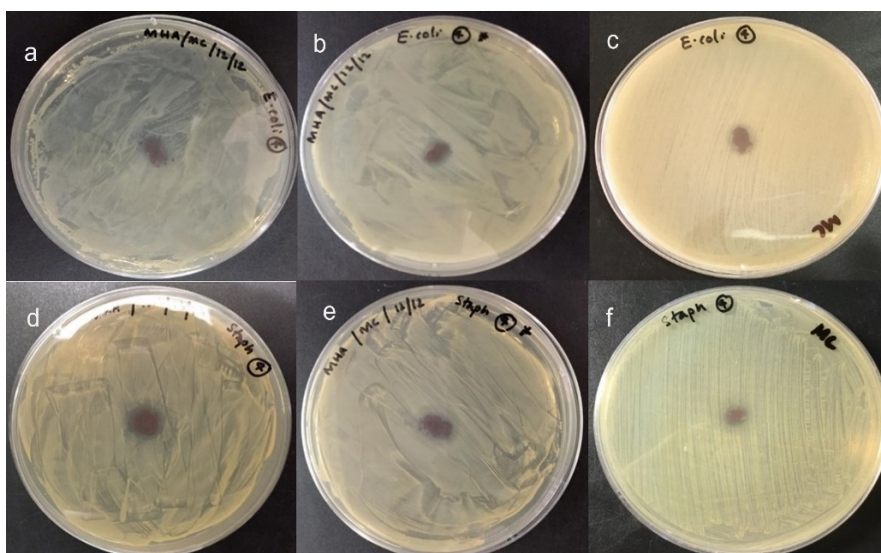


**Figure 1.** Random samples of modified hematite nanomaterials prepared with (a) C4 precursor concentration, at drying temperature 1 (100°C), (b) C4 precursor concentration, at drying temperature 2 (120°C), (c) C4 precursor concentration, at drying temperature 3 (140°C) showing the respective inhibition zones against *Escherichia coli*. Random samples of modified hematite nanomaterials prepared with (d) C4 precursor concentration, at drying temperature 1 (100°C), (e) C4 precursor concentration, at drying temperature 2 (120°C), (f) C4 precursor concentration, at drying temperature 3 (140°C) showing the respective inhibition zones against *Staphylococcus aureus*.

**Table 1.** Antibacterial efficacy of the nanoparticles prepared with different concentrations at different temperatures.

Temperature	Concentration	Inhibition zone size <i>E. coli</i> (mm)	Inhibition zone size <i>S. aureus</i> (mm)
100°C	C1	9.5	12.0
	C2	No growth on NPs	9.5
	C3	9.5	No growth on NPs
	<b>C4</b>	<b>10.0</b>	<b>12.0</b>
	C5	No growth on NPs	No growth on NPs
120°C	C1	9.5	9.5
	C2	10.0	10.0
	C3	No growth on NPs	No growth on NPs
	<b>C4</b>	<b>11.0</b>	<b>12.0</b>
	C5	No growth on NPs	No growth on NPs
140°C	C1	11.0	12.0
	C2	9.5	No growth on NPs
	C3	No growth on NPs	No growth on NPs
	<b>C4</b>	<b>12.0</b>	<b>12.0</b>
	C5	No growth on NPs	No growth on NPs

Species" (ROS). These "ROS" can easily degrade organic matter, and this might be the reason to have effective inhibition zones around the samples modified with C4 concentration, where the concentration is lower than that of C1, C2 and C3. Even though C5 has the least concentration, it does not show a higher antimicrobial ability, and this indicates that after a certain size the material fails to generate ROSs at a higher availability.

However, the curing temperature did not change the inhibition zone diameters significantly. Therefore, the C4 concentration was selected as the optimum concentration and 120°C as the preferred temperature.

2) Antibacterial Activity of modified hematite nanomaterials with and without washing.

3) Antibacterial Activity of modified hematite nanomaterials (washed) after 3 months.

The above results in **Figure 2** and **Table 2** specify the inhibition zone sizes around the modified material. It is evident that the hematite nanostructures have the desired property against both Gram-positive and Gram-negative bacterial strains regardless of having been washed or not. This procedure had to be delivered to confirm that the antimicrobial activity of the modified material does not have any relation to having NaCl, generated in the reaction. No bacterial growth was apparent around the material, and they have very distinguishable inhibition zones.

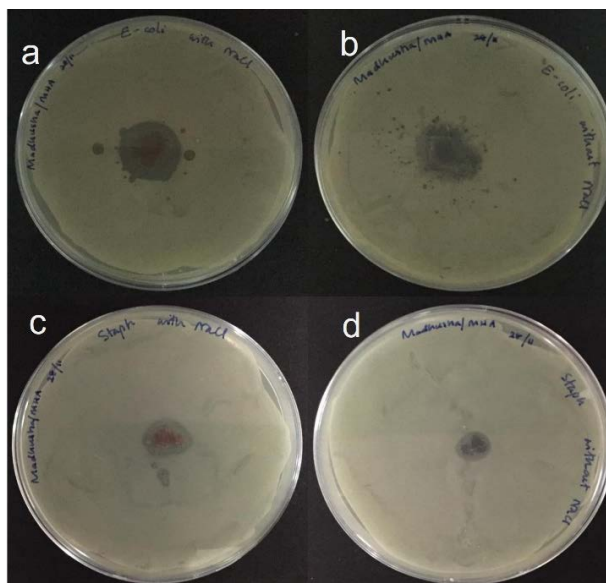


**Figure 2.** Modified hematite nanomaterials prepared with (a) C4 precursor concentration, at drying temperature 2 (120°C) without washing (b) C4 precursor concentration, at drying temperature 2 (120°C) with washing, showing the respective inhibition zones against *Escherichia coli*. Modified hematite nanomaterials prepared with (c) C4 precursor concentration, at drying temperature 2 (120°C) without washing (d) C4 precursor concentration, at drying temperature 2 (120°C) with washing, showing the respective inhibition zones against *Staphylococcus aureus*.

**Table 2.** Antibacterial efficacy of the nanoparticle at C4/T2 in different conditions.

Condition	Inhibition zone size <i>E. coli</i> (mm)	Inhibition zone size <i>S. aureus</i> (mm)
With NaCl	18.0	16.0
Without NaCl	12.0	12.0
After 3 months without NaCl	12.0	12.0

The reason to have comparatively bigger inhibition zones for the samples with NaCl (without washing) may be due to the ability of NaCl to effectively pull-out water from bacterial cells by osmosis. All the samples without NaCl show similar strengths of antibacterial activity. The property remains the same even after three months of production and the intensities are still the same (Figure 3 and Table 2). This confirms the consistency and the durability of the modified materials.

#### 4) Antifungal Activity of modified hematite nanomaterials (washed) after 3 months

To verify the antimicrobial property of the modified materials in a more general manner they were tested against *Candida albicans*, in the prospect of examining their antifungal activity. However, in contrast to antibacterial properties, antifungal properties did not differ with or without NaCl. Even if, no fungal population was distinct around or on the modified materials. Generally, it is hard to inhibit fungal growth because unlike bacteria, fungi are eukaryotes.

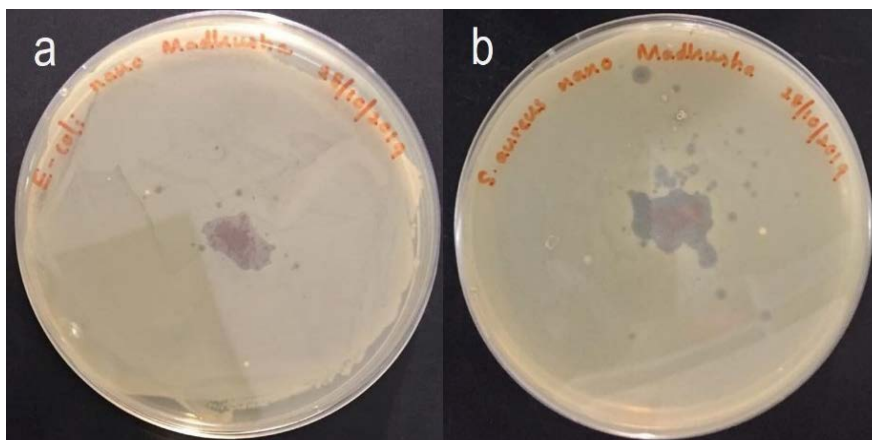


**Figure 3.** Modified hematite nanomaterials (washed) prepared with (a) C4 precursor concentration, at drying temperature 2 (120°C) showing the respective inhibition zones against *Escherichia coli* after three months of development. (b) C4 precursor concentration, at drying temperature 2 (120°C) showing the respective inhibition zones against *Staphylococcus aureus* after three months of development.

There might be limitations in killing fungal cells. Still, the information from the above images in **Figure 4** and **Table 3**, ratify that the material can restrain fungal growth on it.

## Characterization of the Iron Oxide Nanoparticle

### SEM Imaging

The scanning electron microscopy was used to characterize the mean particle size and morphology of iron oxide nanoparticles.

According to the above SEM image in **Figure 5**, it is distinct that some of the hematite particles are around 100 nm in size or less than that. It confirms that the describing method is viable in synthesizing hematite nanostructures. These nano structures have enhanced band gap energies which can cause a higher production of ROS, that ultimately destroys microbes. The above SEM image corresponds to the hematite nano-structures synthesized with C4 precursor concentration, at drying temperature 2 (120°C). As the materials produced under these conditions have the highest anti-microbial activities, they have been used in SEM imaging.

As shown in **Figure 6**, the major diffraction peak at 35.617° (110) in addition to minor peaks at 24.87° (012), 33.07° (104), 42.08° (113), 51.18° (024), 53.52° (116) and, 57.46° (018) confirm the spinel structure of iron oxide ( $\alpha$ -Fe<sub>2</sub>O<sub>3</sub>). For further confirmation, we have considered the  $2\theta$  value of the (110) peak. As reported in various literature, the standard values of this peak (110) for hematite are at 35° [17]. Additionally, the analysis of  $\alpha$ -Fe<sub>2</sub>O<sub>3</sub> XRD patterns using X' pert high score software with search and match option reveals that synthesized NPs have Fe<sub>2</sub>O<sub>3</sub> crystals (JCPDS reference code-75-0033). The crystallite size of the nano-materials was calculated from its higher intense peak in the XRD patterns using Debye Scherrer's equation and the estimated average crystallite size was 36.74 nm.



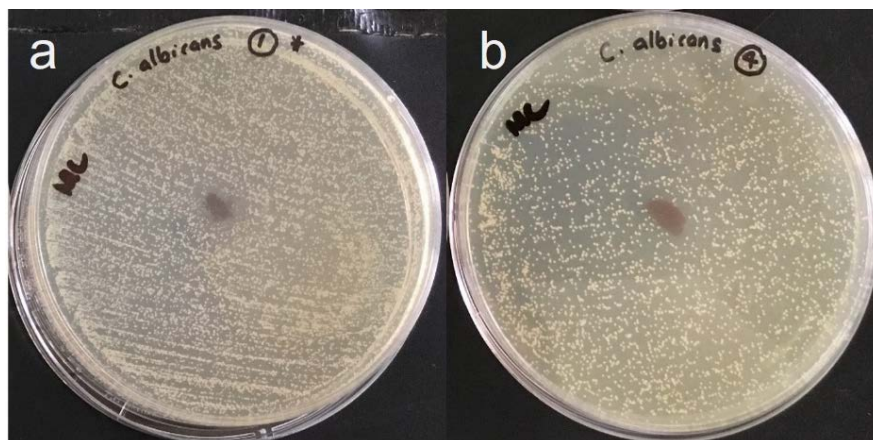


**Figure 4.** Random samples of modified hematite nanomaterials prepared with (a) C4 precursor concentration, at drying temperature 2 (120°C), (b) C3 precursor concentration, at drying temperature 2 (120°C), showing respective inhibition zones against *Candida albicans*.

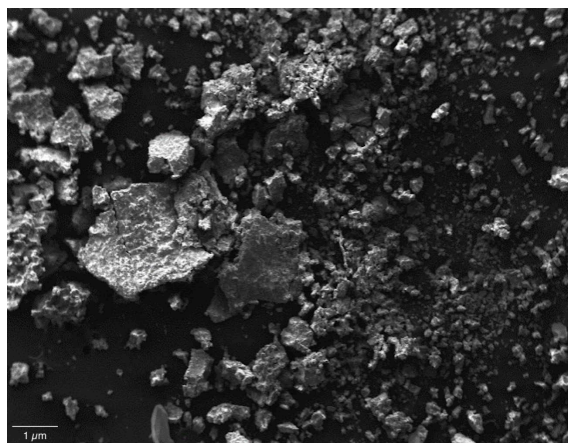


**Figure 5.** SEM image of hematite ( $\alpha\text{-Fe}_2\text{O}_3$ ) nano-structures prepared with C4 precursor concentration, at drying temperature 2 (120°C).

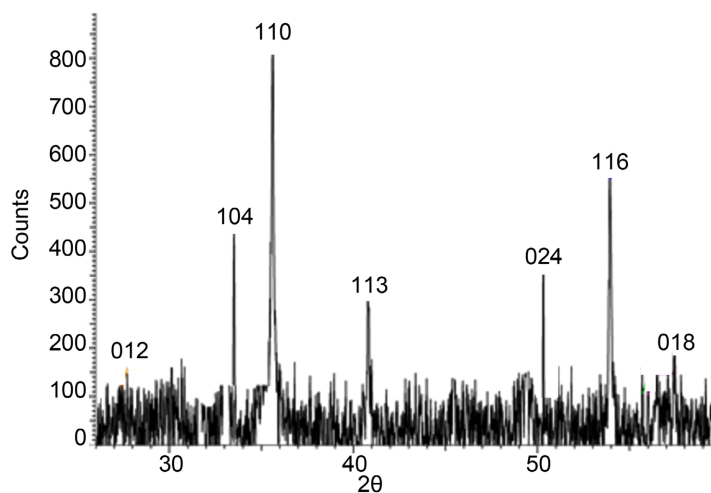


**Figure 6.** XRD pattern of hematite nanostructures prepared with C4 precursor concentration, at drying temperature 2 (120°C).

**Table 3.** Antifungal efficacy of the nanoparticles prepared with different concentrations at 120°C.

Temperature	Concentration	Inhibition zone size <i>Candida albicans</i>	Washed/without washed
120°C	C1	No growth on NPs	Washed
	C2	No growth on NPs	Washed
	C3	9.6	Washed
	<b>C4</b>	<b>9.8</b>	Washed
	C5	No growth on NPs	washed
120°C	C4	10.0	Without washed

#### 4. Conclusion

Hematite nanomaterials were successfully synthesized using the waste effluent of galvanizing bath obtained from LTL Galvanizers Pvt. Ltd, Sapugaskanda, Sri Lanka, with a chemical precipitation method. The increased surface area of these nanomaterials, along with the increased band gap, provided requiring conditions to manufacture ROS which are responsible for the destruction of microbial cells. The analysis of nanomaterials with XRD spectroscopy and SEM showed that they were highly mono-crystalline and in the nano range. Synthesized hematite nanomaterials not only prevent the growth of bacteria but also kill the ones which come into contact. The samples modified using the C4 precursor concentration, at drying temperature 2 (120°C) showed the biggest inhibition zones. All the samples showed excellent anti-bacterial and anti-fungal properties and the material was incapable of inhibiting the growth of both Gram-positive and Gram-negative bacteria. The durability of the manufactured nano materials was excellent which has been confirmed by the antimicrobial activity of the samples tested after three months of production. The method is a time-efficient, environmentally friendly, cost-effective and industrially viable way to manufacture antimicrobial hematite ( $\alpha$ -Fe<sub>2</sub>O<sub>3</sub>) nanomaterials. The process has been used to manufacture those nanomaterials on the bulk scale and the resulted pigment was used in a commercial project to manufacture an iron oxide-based antimicrobial paint.

#### Conflict of Interest Statement

On behalf of all authors, the corresponding author states that there is no conflict of interest.

#### References

- [1] Yan, J.B., Liew, J.R., Zhang, M.H. and Wang, J.Y. (2014) Mechanical Properties of Normal Strength Mild Steel and High Strength Steel S690 in Low Temperature Relevant to Arctic Environment. *Materials & Design*, **61**, 150-159. <https://doi.org/10.1016/j.matdes.2014.04.057>
- [2] Corradi, M., Di Schino, A., Borri, A. and Rufini, R. (2018) A Review of the Use of

- Stainless Steel for Masonry Repair and Reinforcement. *Construction and Building Materials*, **181**, 335-346. <https://doi.org/10.1016/j.conbuildmat.2018.06.034>
- [3] Wang, R., Sheno, R.A. and Sobey, A. (2018) Ultimate Strength Assessment of Plated Steel Structures with Random Pitting Corrosion Damage. *Journal of Constructional Steel Research*, **143**, 331-342. <https://doi.org/10.1016/j.jcsr.2018.01.014>
- [4] Nguyen, M.N., Wang, X. and Leicester, R.H. (2013) An Assessment of Climate Change Effects on Atmospheric Corrosion Rates of Steel Structures. *Corrosion Engineering, Science and Technology*, **48**, 359-369. <https://doi.org/10.1179/1743278213Y.0000000087>
- [5] Shibli, S.M.A., Meena, B.N. and Remya, R. (2015) A Review on Recent Approaches in the Field of Hot Dip Zinc Galvanizing Process. *Surface and Coatings Technology*, **262**, 210-215. <https://doi.org/10.1016/j.surfcoat.2014.12.054>
- [6] Bush, G.W. (1989) Developments in the Continuous Galvanizing of Steel. *The Journal of the Minerals*, **41**, 34-36. <https://doi.org/10.1007/BF03220301>
- [7] Bennett, P.B. (2006) Ion-Channel Drug Screening Galvanized. *Nature Biotechnology*, **24**, 415-416. <https://doi.org/10.1038/nbt0406-415>
- [8] Savage, T. (1995) Galvanizing—Past, Present and Future. *Anti-Corrosion Methods and Materials*, **42**, 23-25. <https://doi.org/10.1108/eb007371>
- [9] Ozturk, F., Evis, Z. and Kilic, S. (2017) Hot-Dip Galvanizing Process. *Comprehensive Materials Finishing*, **3**, 178-190. <https://doi.org/10.1016/B978-0-12-803581-8.09175-X>
- [10] Afena, A., Boateng, D., Darkwah, L. and Adjaottor, A. (2021) Decolourisation of Textile Wastewater by Dye Degrading Microorganisms Isolated from Textile Effluent. *Journal of Environmental Protection*, **12**, 767-783. <https://doi.org/10.4236/jep.2021.1210046>
- [11] Watt, J., Cheong, S. and Tilley, R.D. (2013) How to Control the Shape of Metal Nanostructures in Organic Solution Phase Synthesis for Plasmonics and Catalysis. *Nano Today*, **8**, 198-215. <https://doi.org/10.1016/j.nantod.2013.03.001>
- [12] Sánchez-López, E., Gomes, D., Esteruelas, G., Bonilla, L., Lopez-Machado, A.L., Galindo, R., Cano, A., Espina, M., Ettcheto, M., Camins, A. and Silva, A.M. (2010) Metal-Based Nanoparticles as Antimicrobial Agents: An Overview. *Nanomaterials*, **10**, Article 292. <https://doi.org/10.3390/nano10020292>
- [13] Naseem, T. and Farrukh, M.A. (2015) Antibacterial Activity of Green Synthesis of Iron Nanoparticles Using *Lawsoniainermis* and *Gardenia Jasminoides* Leaves Extract. *Journal of Chemistry*, **2015**, Article ID: 912342. <https://doi.org/10.1155/2015/912342>
- [14] Chatterjee, K., Sarkar, S., Jagajjanani Rao, K. and Paria, S. (2014) Core/Shell Nanoparticles in Biomedical Applications. *Advances in Colloid and Interface Science*, **209**, 8-39. <https://doi.org/10.1016/j.cis.2013.12.008>
- [15] Mahdavi, M., et al. (2013) Synthesis, Surface Modification and Characterisation of Biocompatible Magnetic Iron Oxide Nanoparticles for Biomedical Applications. *Molecules*, **18**, 7533-7548. <https://doi.org/10.3390/molecules18077533>
- [16] Shahzadi, S., Zafar, N. and Sharif, R. (2018) Antibacterial Activity of Metallic Nanoparticles. *Bacterial Pathogenesis and Antibacterial Control*, **51**, 51-94. <https://doi.org/10.5772/intechopen.72526>
- [17] Hjiri, M. (2020) Highly Sensitive NO<sub>2</sub> Gas Sensor Based on Hematite Nanoparticles Synthesized by Sol–Gel Technique. *Journal of Materials Science: Materials in Electronics*, **31**, 5025-5031. <https://doi.org/10.1007/s10854-020-03069-4>